Accepted Manuscript

Comparison between porphin, chlorin and bacteriochlorin derivatives for photodynamic therapy: Synthesis, photophysical properties, and biological activity

Wei Zhu, Ying-Hua Gao, Ping-Yong Liao, Dan-Ye Chen, Ning-Ning Sun, Phuong Anh Nguyen Thi, Yi-Jia Yan, Xiao-Feng Wu, Zhi-Long Chen

PII: S0223-5234(18)30867-5

DOI: 10.1016/j.ejmech.2018.10.005

Reference: EJMECH 10791

To appear in: *European Journal of Medicinal Chemistry*

Received Date: 7 September 2018

Revised Date: 28 September 2018

Accepted Date: 1 October 2018

Please cite this article as: W. Zhu, Y.-H. Gao, P.-Y. Liao, D.-Y. Chen, N.-N. Sun, P.A. Nguyen Thi, Y.-J. Yan, X.-F. Wu, Z.-L. Chen, Comparison between porphin, chlorin and bacteriochlorin derivatives for photodynamic therapy: Synthesis, photophysical properties, and biological activity, *European Journal of Medicinal Chemistry* (2018), doi: https://doi.org/10.1016/j.ejmech.2018.10.005.

Table of Contents (TOC) Graphic

Three series of porphins (**P1-4**), chlorins (**C1-4**) and bacteriochlorins (**B1-4**) were synthesized. Among them, **B2** is a powerful and promising antitumor PS for photodynamic therapy.

Comparison between porphin, chlorin and bacteriochlorin derivatives for photodynamic therapy: synthesis, photophysical properties, and biological activity

Wei Zhu[1], Ying-Hua Gao[1], Ping-Yong Liao[1], Dan-Ye Chen[1], Ning-Ning Sun[1], Phuong Anh Nguyen Thi[1], Yi-Jia Yan[2,3], Xiao-Feng Wu[3]* and Zhi-Long Chen[1]*

[1] *Department of pharmaceutical Science & Technology, College of Chemistry and Biology, Donghua University, Shanghai 201620, China*

[2] *Ningbo Dongmi Pharmaceutical Co., Ltd, Ningbo 315899, China*

[3] *Shanghai Xianhui Pharmaceutical Co., Ltd, Shanghai 200433, China*

KEYWORDS：porphin, chlorin, bacteriochlorin, photodynamic therapy, antitumor

ABSTRACT: The development of novel photosensitizers is a challenging task for photodynamic therapy (PDT). Twelve novel photosensitizers (PSs), including porphins (**P1-4**), chlorins (**C1-4**) and bacteriochlorins (**B1-4**) were synthesized. The bacteriochlorins exhibited the longest absorption wavelength (λ_{max}= 736 nm), which is higher than that of porphins (λ_{max} = 630 nm) and chlorins (λ_{max} = 644 nm). In vitro photodynamic activities on Eca-109 human

esophageal carcinoma cells were evaluated by standard assays and all PSs showed photodynamic activity. Among them, **B2** displayed the highest phototoxicity and the lowest dark toxicity. In addition, **B2** exhibited best photodynamic antitumor efficacy on BALB/c nude mice bearing Eca-109 cells tumor. Therefore, **B2** is a powerful and promising antitumor photosensitizer for PDT.

1. Introduction

Cancer has been seriously threatening human health in contemporary society [1-3]. Diagnosis and treatment of cancer have become the most pressing concern. PDT has emerged as an alternative modality for specifically killing malignant tissues, especially for some localized and superficial tumors [4-6]. The design and synthesis of novel photosensitizers (PSs) are central to the development of efficient PDT modalities, particularly the reduction of the doses of drug and photoirradiation by increasing photocytotoxicity, selective accumulation in the tumor, and rapid clearance after treatment to reduce side effects such as prolonged skin sensitivity [7-8].

Commercial photofrin II is a porphyrin-based photosensitizer that has been commercially produced and approved in several countries for the PDT [4, 9-11]. However, it still suffered from several drawbacks such as chemical heterogeneity, poor tissue penetration due to its limited maximum absorption wavelength, weak absorption at therapeutic wave length (630 nm), and prolonged cutaneous photosensitivity caused by its slow elimination in normal tissue [12]. For these reasons, several PSs possessing stronger and red-shifted absorption within the therapeutic window have been investigated in PDT (**Figure 1**). Compared to porphins, chlorin-type PSs are receiving considerable attention owing to their intense absorption in near infrared region (≥ 650 nm), which are relatively harmless and penetrate deeply in biological tissues [13-15]. Among them, talaporfin [16-17] (mono-L-aspartyl chlorin e6), and temoporfin [18-19] (m-THPC) were approved for PDT treatment. Bacteriochlorins are a class of tetrapyrrole macrocycles with two

unsaturated pyrrolic rings. This ring structure occurs naturally in photosynthetic pigments (bacteriochlorophylls a and b) from purple photosynthetic bacteria of the orders *Rhodospirillales and Rhizobiales* [20]. Bacteriochlorin-type PSs received intensive attention due to their advantage of maximum absorption in near infrared region (740 - 780 nm), enabling deep penetration of light in animal tissues i.e. ~8 mm [21-22]. Pd-bacteriopheophorbide, padeliporfin and redaporfin have entered clinical trials [23-28]. However, many naturally occurring and naturally derived bacteriochlorins were notoriously difficult to extract from a bacterial culture with a low yield.

Banfi et al. had reported a series of diphenylporphins and one diphenylchlorin compound without substituents [29]. Besides, di(3,5-dihydroxyphenyl)chlorin was reported by Patrice et al. as an excellent PS [30]. The comparison between porphin, chlorin and bacteriochlorin with the same substituents in the benzene ring has not been reported till now. In the present study, 12 novel PSs, including porphins (**P1-4**), chlorins (**C1-4**) and bacteriochlorins (**B1-4**) were synthesized and characterized. Their photophysical properties, subcellular localization, photodynamic activities in vitro and in vivo were reported herein.

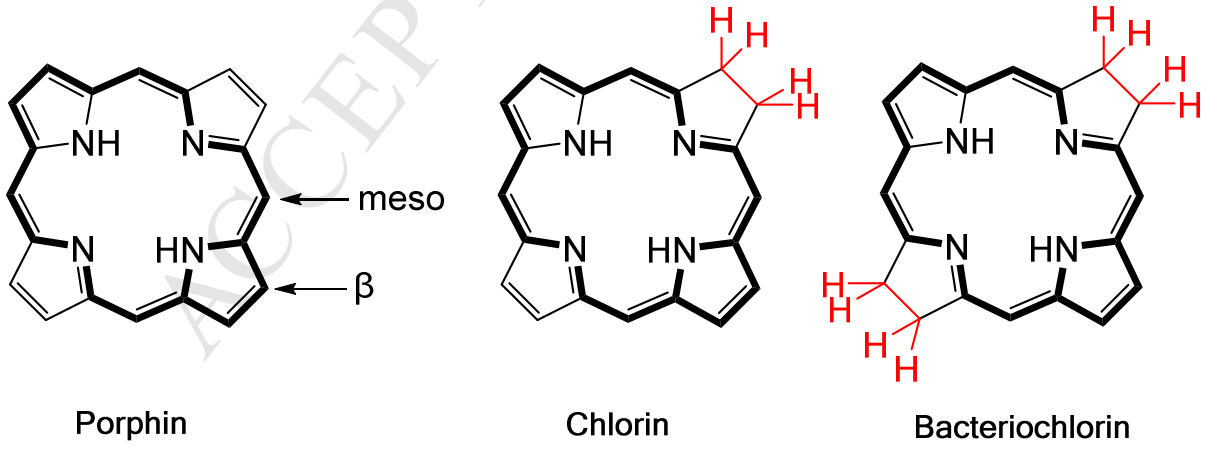

Figure 1. The general structure of tetrapyrrole derivatives

2. Results and discussion

2.1. Chemistry

A number of different procedures have been reported for the synthesis of 5,15-diarylporphins [31-32], mostly based on a (2 + 2)-type condensation in which two dipyrrolic derivatives incorporating one type of carbon bridge are fused together, thereby forming the other type of carbon bridge, the intermediate is then oxidized in situ to the final porphin [33-34]. The aromatic aldehyde monomers (**2a-c)** were synthesized according to literature procedures [35-38]. Symmetric diarylporphins (**3a-d**) were synthesized via acid-catalyzed mixed condensation of dipyrromethane with aromatic aldehydes, following the general procedure described by Lindsey and co-workers [39]. The porphyrinogen intermediate was oxidized to porphin with 2,3-dichloro-5,6-dicyano-1,4-benzoquinone (DDQ). Then diarylporphins (**3a-d**) were treated with 2 N KOH, and hydrolyzed to give the target compounds (**P1-4**). The overall yields of the products (43.4% - 53.1%) are excellent (**Scheme 1**).

Scheme 1 Synthesis of the porphins (**P1-4**) [a]

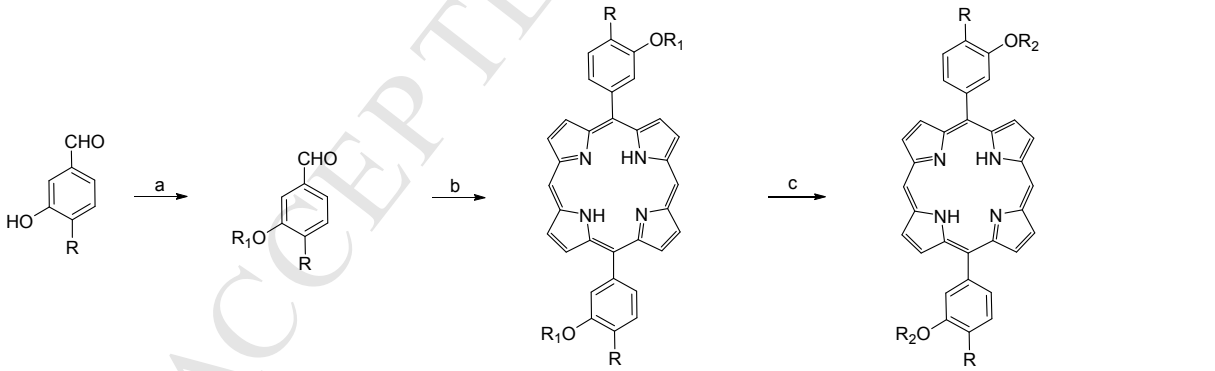

1a: R=-H
1b: R=-OMe

2a: R=-H, R_1=-CH_2COOEt;
2b: R=-H, R_1=-$CH_2CH_2CH_2COOEt$;
2c: R=-OMe, R_1=-CH_2COOEt;
2d: R=-OMe, R_1=-$CH_2CH_2CH_2COOEt$.

3a: R=-H, R_1=-CH_2COOEt;
3b: R=-H, R_1=-$CH_2CH_2CH_2COOEt$;
3c: R=-OMe, R_1=-CH_2COOEt;
3d: R=-OMe, R_1=-$CH_2CH_2CH_2COOEt$.

P1: R=-H, R_2=-CH_2COOH;
P2: R=-H, R_2=-$CH_2CH_2CH_2COOH$;
P3: R=-OMe, R_2=-CH_2COOH;
P4: R=-OMe, R_2=-$CH_2CH_2CH_2COOH$.

[a] Reagents and reaction conditions: (a) ethyl bromoacetate or ethyl 4-bromobutyrate, K_2CO_3, DMF, 100 □, 9 h; (b) i) dipyrromethane, TFA, DCM, 12 h; ii) DDQ, Et_3N, 3 h; (c) 2 N KOH, MeOH/THF, reflux, 12 h.

The synthetic route of the chlorins (**C1-4**) is shown in **Scheme 2**. According to the method of Whitlock and co-workers [40], the diarylporphins were reduced with diimide. Briefly, the compounds (**3a-d)** were treated with *p*-toluenesulfonyl hydrazide, and then *p*-chloranil was added in portions until the absorption band at 734 nm disappeared. The chlorins (**4a-d**) were treated with 2 N KOH, and hydrolyzed to give the target compounds (**C1-4**).

Scheme 2 Synthesis of the chlorins (**C1-4**) [a]

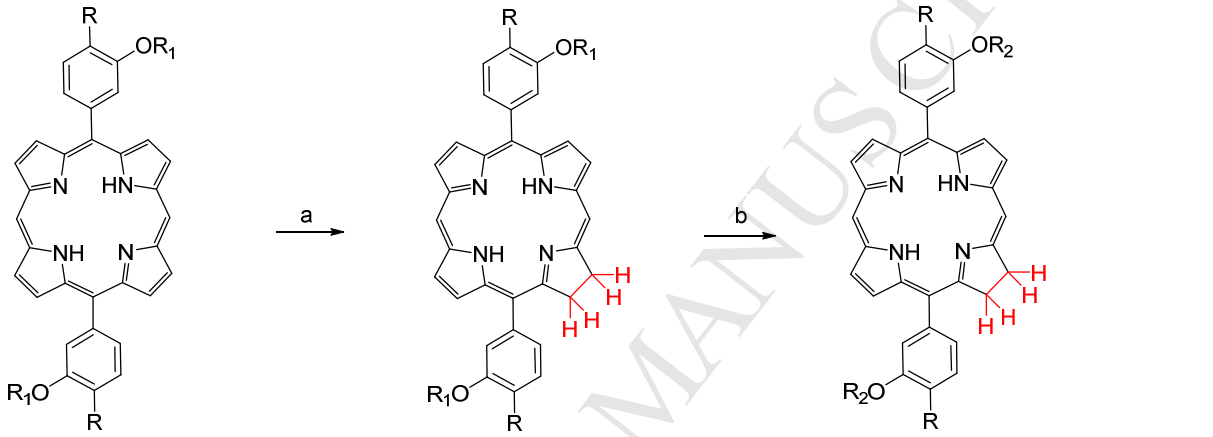

3a: R=-H, R_1=-CH_2COOEt;
3b: R=-H, R_1=-$CH_2CH_2CH_2COOEt$;
3c: R=-OMe, R_1=-CH_2COOEt;
3d: R=-OMe, R_1=-$CH_2CH_2CH_2COOEt$.

4a: R=-H, R_1=-CH_2COOEt;
4b: R=-H, R_1=-$CH_2CH_2CH_2COOEt$;
4c: R=-OMe, R_1=-CH_2COOEt;
4d: R=-OMe, R_1=-$CH_2CH_2CH_2COOEt$.

C1: R=-H, R_1=-CH_2COOH;
C2: R=-H, R_1=-$CH_2CH_2CH_2COOH$;
C3: R=-OMe, R_1=-CH_2COOH;
C4: R=-OMe, R_1=-$CH_2CH_2CH_2COOH$.

[a] Reagents and reaction conditions: (a) i) *p*-$TsNHNH_2$, K_2CO_3, pyridine, reflux, 8 h; ii) *p*-chloranil, ethyl acetate, rt.; (b) 2 N KOH, THF/MeOH, reflux, 12 h.

Compared with the chlorins (**C1-4**), the synthesis of the bacteriochlorins (**B1-4**) was quite difficult, requiring a long reaction time and a large amount of *p*-toluenesulfonyl hydrazine than the similar method described for chlorin [40]. Due to the relative unstability of the bacteriochlorins, their post-treatment need to be very careful and quick in the preparation process. The yields of the compounds (**5a-d**) ranged from 18% to 35%. The bacteriochlorins (**5a-d**) were treated with 2 N KOH, and hydrolyzed to give the target bacteriochlorins (**B1-4**) (**Scheme 3**). The identities of porphins (**P1-4**), chlorins (**C1-4**), and bacteriochlorins (**B1-4**) were elucidated by ^{1}H NMR, ^{13}C NMR and HR-MS (**Figure S1-24**).

Scheme 3 Synthesis of the bacteriochlorins (**B1-4**) [a]

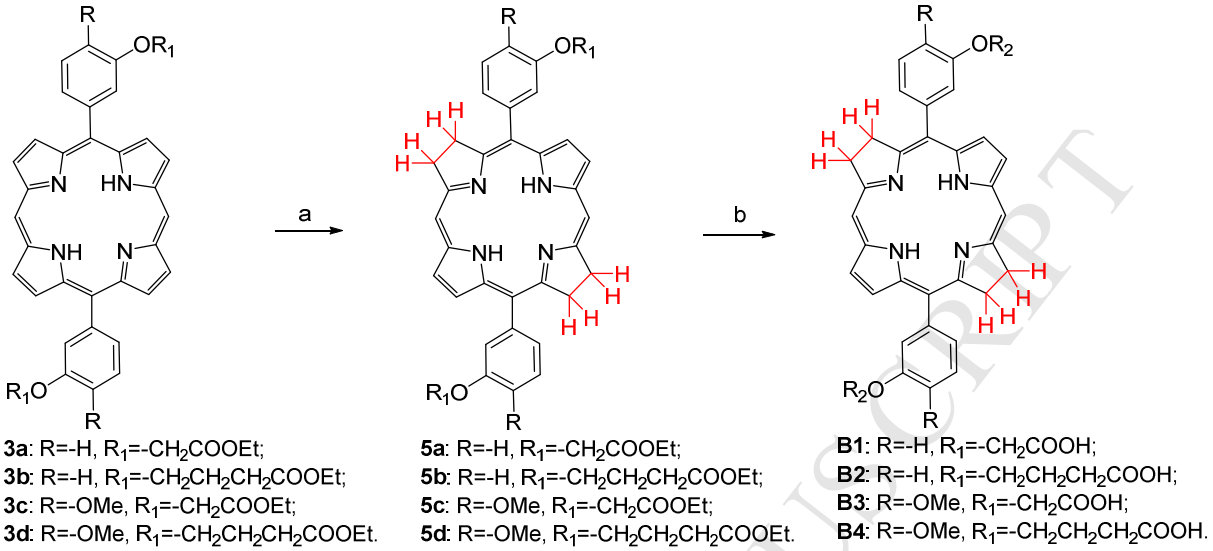

3a: R=-H, R_1=-CH_2COOEt;
3b: R=-H, R_1=-$CH_2CH_2CH_2COOEt$;
3c: R=-OMe, R_1=-CH_2COOEt;
3d: R=-OMe, R_1=-$CH_2CH_2CH_2COOEt$.

5a: R=-H, R_1=-CH_2COOEt;
5b: R=-H, R_1=-$CH_2CH_2CH_2COOEt$;
5c: R=-OMe, R_1=-CH_2COOEt;
5d: R=-OMe, R_1=-$CH_2CH_2CH_2COOEt$.

B1: R=-H, R_1=-CH_2COOH;
B2: R=-H, R_1=-$CH_2CH_2CH_2COOH$;
B3: R=-OMe, R_1=-CH_2COOH;
B4: R=-OMe, R_1=-$CH_2CH_2CH_2COOH$.

[a] Reagents and reaction conditions: (a) *p*-$TsNHNH_2$, pyridine, K_2CO_3, reflux 12 h. (b) 2 N KOH, THF/MeOH, reflux, 18 h.

2.2. UV-visible absorption and fluorescence spectra.

Due to the four conjugated pyrrole rings, porphins possess high rigidness and good coplanarity, exhibiting strong UV-visible absorption and fluorescence at room temperature [41]. Schematic energy level diagram for highest occupied orbitals (HOMO) and lowest unoccupied orbitals (LUMO) of parent porphin, chlorin and bacteriochlorin are illustrated in **Figure 2**. Theoretical calculations of molecular orbitals for porphin, chlorin and bacteriochlorin show that the LUMO energies are not very sensitive to the number of π electrons reduced from 22 to 20 and 18 respectively [42]. Compounds **P2**, **C2** and **B2** as examples, their UV-vis absorption spectra were shown in **Figure 3** at a concentration of 8 μM. The UV-vis absorption spectra of **P1-4**, **C1-4** and **B1-4** were shown in concentrations ranging from 1 μM to 10 μM in supplemental material (**Figure S25)**. The fluorescence excitation and emission spectra of **P1-4**, **C1-4** and **B1-4** were shown in **Figure 4** and **Table 1**. Interestingly, the maximum absorption wavelength of bacteriochlorin is about 736 nm which might be able to treat deeper tumors. The

emission wavelength of bacteriochlorin is better than both porphin and chlorin, and evenly centered at ~740 nm. This provides the possibilities of bacteriochlorins as near infrared (NIR) fluorescence imaging agents.

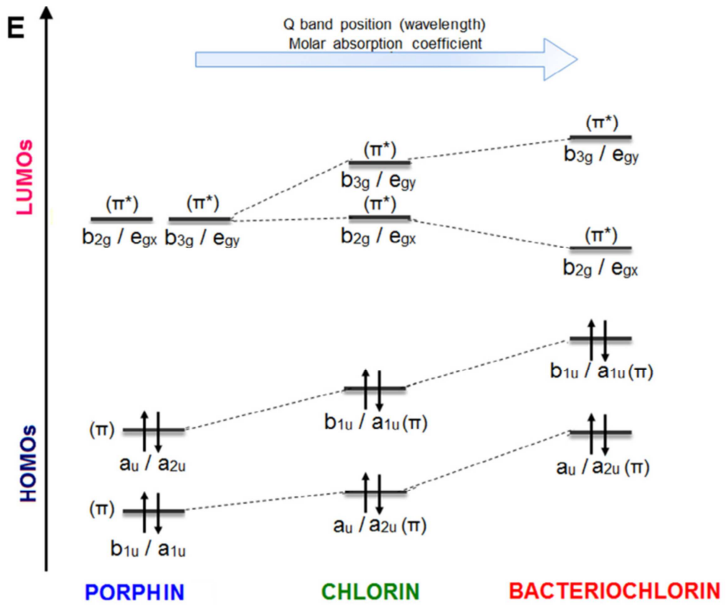

Figure 2. The highest occupied orbitals (HOMO) and lowest unoccupied orbitals (LUMO) of porphin, chlorin and bacteriochlorin

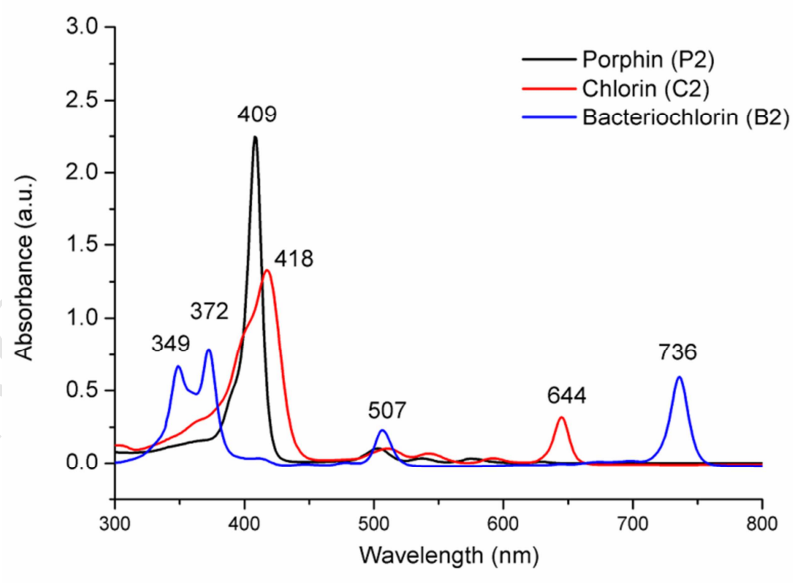

Figure 3. Absorption spectra of **P2**, **C2** and **B2** in DMSO at the concentration of 8 μM.

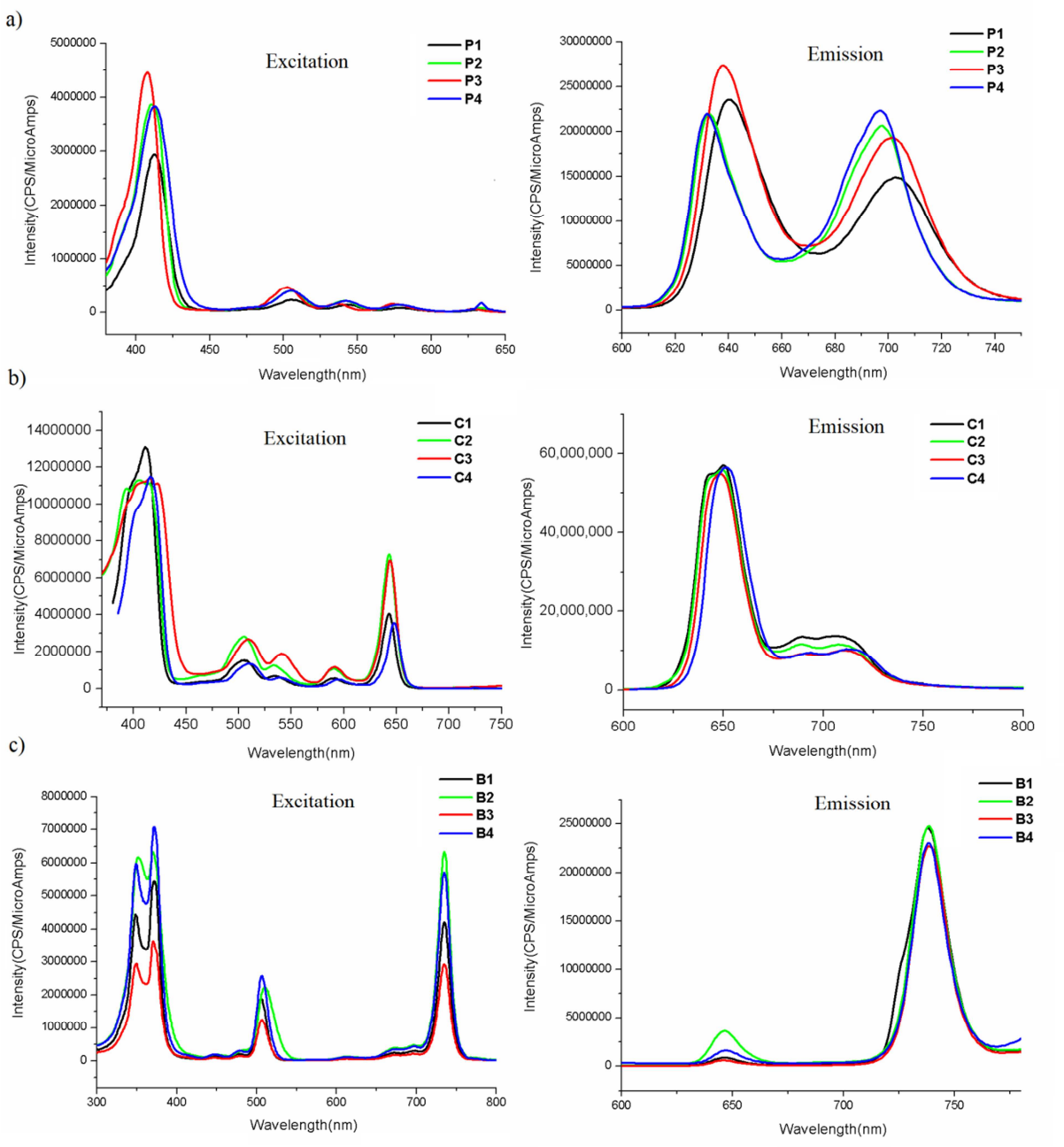

Figure 4. Fluorescence excitation and emission spectra of **P1-4**, **C1-4** and **B1-4** in DMSO at the concentration of 4 μM.

Table 1. Photophysical data[a] for compounds **P1-4**, **C1-4** and **B1-4** at T = 293 K.

Compds	Absorption λ_{max}(nm)[b] ($\varepsilon\times10^4$ $M^{-1}\cdot cm^{-1}$)				Emission λ_{max} (nm)[b]		Stokes shift (nm)
	Soret	ε(Soret)	Q_y	ε(Q_y)	Excitation	Emission	
P1	408	37	630	0.375	408	633	3
P2	406	41	630	0.20	406	632	2
P3	415	14.22	633	0.72	415	644	11
P4	413	23.22	634	0.40	413	639	5
C1	411	18.35	644	4.20	411	649	5
C2	418	13.97	645	3.40	418	649	4
C3	411	19.97	644	4.15	411	650	6
C4	411	12.20	644	4.05	412	651	2
B1	349/373	5.85/7.15	736	5.20	373	738	2
B2	349/373	12.97/58.54	736	11.02	373	740	2
B3	352/373	7.47/6.92	736	6.02	373	738	2
B4	352/373	3.52/3.7	736	3.72	373	738	2

[a] Absorption, excitation and fluorescence emission wavelength, stokes shift. [b] Solvent, DMSO.

2.3. Singlet oxygen quantum yield.

As one of three elements of PDT, ROS are the key cytotoxic intermediates of PDT [43]. Therefore, the efficiency of the ROS generation upon irradiation is an important measure for the cytotoxicity of PSs. The quantum yield of ROS generated by photosensitization of new PSs was determined (**Figure S26**). The quantum yield of singlet oxygen value was determined by using 1, 3- diphenylisobenzofuran (DPBF) as the scavenger. After the data were plotted as k= -ln ($DPBF_t/DPBF_0$)/t, straight lines were obtained for the sensitizers, and the slope for each compound was obtained after fitting with a linear function. **Table 2** lists singlet oxygen

generation (ROS) rates. From holistic comparison, bacteriochlorin was significantly better than chlorin and porphin. As shown in **Table 2**, the results indicate that **P3** displayed the highest ROS yield. Meanwhile, **P2** and **P4** were nearly similar and **P1** was the worst in the porphin series. Among chlorins (**C1-4**), the observed order is **C2** > **C4** > **C3** > **C1**. Significantly, the ROS yield of bacteriochlorins (**B1-4**) gave the order **B2** > **B4** > **B3** >**B1**.

Table 2 Singlet oxygen generation (ROS) rates of compounds **P1-4**, **C1-4** and **B1-4**[a]

Compds	10^{-2}×k[min^{-1}]	Compds	10^{-2}×k[min^{-1}]	Compds	10^{-2}×k[min^{-1}]
P1	0.829	C1	4.056	B1	30.85
P2	1.928	C2	24.847	B2	69.141
P3	2.406	C3	14.238	B3	38.7
P4	1.681	C4	19.798	B4	48.64

[a] Solvent, DMF

2.4. Cytotoxicity

Effective PS needs to possess high phototoxicity and low dark-toxicity [44]. To investigate the potential of **P1-4**, **C1-4** and **B1-4** in PDT, their dark cytotoxicity and phototoxicity were evaluated in esophageal cancer cells (Eca-109) exposed to various concentrations and light doses (**Figure S27-28**). IC_{50} value is an important index for the evaluation of antitumor activity of drugs. The choice of light dose is based on our previous reports [45-47]. The IC_{50} values of their dark-toxicity and photocytotoxicity irradiated by 16 J•cm^{-2} were shown in **Table 3**. There was almost no dark cytotoxicity observed against Eca-109 cells when exposed up to 10 μM. When the concentration was increased to 20 μM, the survival fraction of Eca-109 cells is approximately 80%. The Nd: YAG laser (λ = 635 nm, 650 nm and 730 nm) was respectively used to irradiate these cells at a light dose of 16 J·cm^{-2}. As shown in **Table 3**, **B2** showed the highest

phototoxicity and the lowest dark toxicity among all the compounds toward Eca-109 cells. Therefore, **B2** was highly cytotoxic to malignant esophageal tumor cells.

Table 3 Dark-toxicity[a] and photocytotoxicity of **P1-4**[b], **C1-4**[c] and **B1-4**[d] in Eca-109 cells

Compds	Dark-toxicity (IC_{50}, μM)	Phototoxicity (IC_{50}, μM)
P1	74.63	9.41
P2	271.24	8.19
P3	157.66	12.50
P4	182.83	10.14
C1	91.76	3.31
C2	＞300	2.65
C3	111.29	3.14
C4	＞300	2.83
B1	162.26	2.62
B2	＞500	2.43
B3	186.75	3.09
B4	＞300	2.47

[a] Without irradiation; [b] The light dose was 16 J•cm^{-2} (λ = 635 nm); [c] The light dose was 16 J•cm^{-2} (λ = 650 nm); [d] The light dose was 16 J•cm^{-2} (λ =730 nm).

2.5. Intracellular localization

The subcellular localization of the PS is of special significance, since it determines the site of primary photodamages and the type of cellular response to the therapy. Cellular structures containing PS would be preferentially damaged upon illumination [48-50]. The preferential sites of subcellular localization of **B2** were evaluated by laser confocal microscopy upon exposure of Eca-109 cells to **B2** (10 μM) for 4 h and staining with Mitro-tracker Green and Lyso-Blue for mitochondria and lysosome, respectively. As shown in **Figure 5,** the merged stained images

revealed the overlaps of **B2** with Mitro-tracker Green (green signal) and Lyso Blue (blue signal), suggesting that the PSs were mainly found in organelles of mitochondria and lysosome.

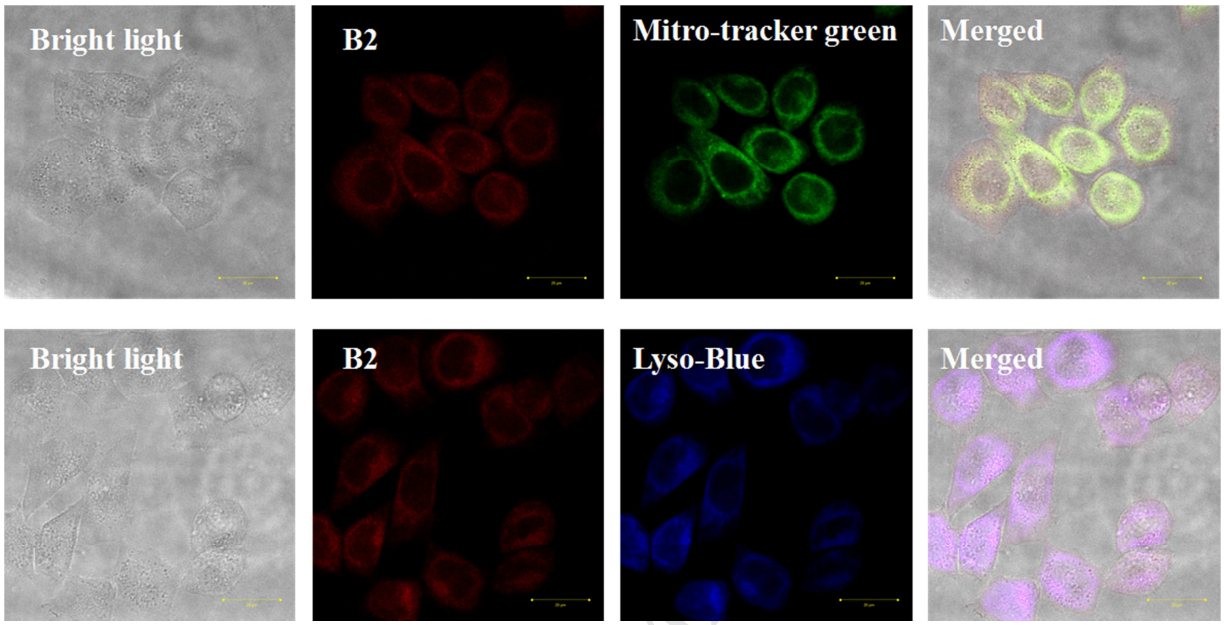

Figure 5. Subcellular location of **B2** in Eca-109 cells at 10 μM for 4 h. Bright field; red fluorescence (**B2**); mitochondria green fluorescence (Mitro-tracker Green) or lysosome (Lyso Blue) and merged images. Scale bar: 20 μm.

2.6. In vivo photosensitizing efficacy

The in vivo therapeutic efficacy of **B2** was evaluated in Eca-109 tumor bearing BABL/c nude mice. The tumor-bearing mice were injected with **B2** (5 mg/kg) via the tail vein, and then irradiated with 350 mW/cm^2 lasers for 5 min (120 J/cm^2, λ = 730 nm) to the tumor area. The mice in PDT group were treated with laser light at 24 h post-injection of the **B2**. The control mice were not subjected to PS or light. After irradiation there was a hemorrhagic and necrotic zone in the tumor sites of PDT group. With swelling, erythema subsided within 2 days. All the tumors were measured in three dimensions every other day for 14 days. As shown in **Figure 6**, the volume growth curves of tumors were provided. The volume of tumors in control, light and

B2 group were larger than that in **B2**-PDT group at the same time. Therefore, the light group has little influence on the growth of tumors, and there is no significant difference among the light irradiation group, **B2** group and the control group. After 14 days, the mean size of tumors only reached 126 ± 25 mm^3 in PDT group, compared to that of 785 ± 37 mm^3 in the control group. These results indicated that **B2** could significantly inhibit the growth of the tumors.

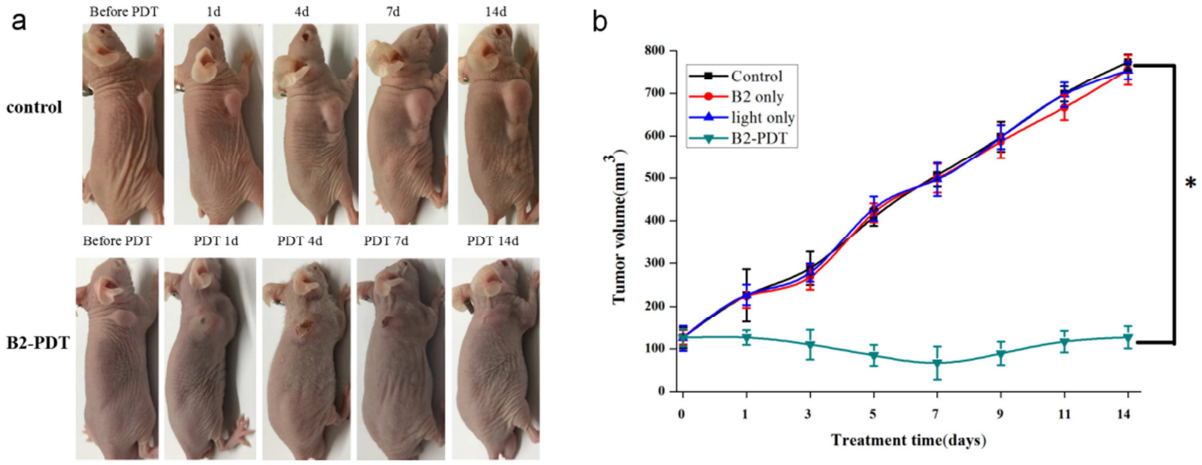

Figure 6. In vivo photosensitizing efficacy of **B2** against Eca-109 tumors (6 mice/group). (**a**). Images of tumor bearing mice before and after treatment; (**b**). Tumor volume at different time after treatment. The data shown are the means ± SD of three independent experiments. *P < 0.05 compared with control group.

3. Conclusions

In summary, twelve novel PSs, including porphins (**P1-4**), chlorins (**C1-4**) and bacteriochlorins (**B1-4**), were synthesized and characterized. The UV-vis absorption results are consistent with the molecular orbital theory. The bacteriochlorins exhibited the longest absorption wavelength (λ_{max} = 736 nm), which is higher than that of porphins (λ_{max} = 630 nm) and chlorins (λ_{max} = 644 nm). In comparison with porphins and chlorins, all bacteriochlorins showed longer absorption and fluorescence emission wavelength. Meanwhile, all three series of PSs can produce ROS and the bacteriochlorins also displayed higher ROS yields. All of the

twelve novel compounds showed photodynamic activity. Among them, **B2** showed the highest phototoxicity and the lowest dark toxicity toward Eca-109 cells. Generally, our data support the fact that **B2** is a promising PS for PDT due to its long absorption and emission wavelength in the phototherapeutic window (absorption λ_{max} = 736 nm, emission λ_{max}= 740 nm), high phototoxicity and low dark-toxicity (phototoxicity IC_{50} = 2.43 μM, dark-toxicity IC_{50} > 500 μM for Eca-109 cells) and excellent in vivo PDT antitumor efficacy.

4. Experimental section

4.1. Chemistry

All solvents and reagents were purchased from commercial suppliers and were used without further purification unless otherwise stated. Melting points were obtained on a "Stuart" Bibby apparatus and uncorrected. ^{1}H-NMR and ^{13}C-NMR spectra were recorded on a Bruker 400 MHz spectrometer. Chemical shifts were reported as δ values relative to the internal standard TMS (Me_4Si). MALDI-TOF mass spectra were recorded on an AB SCIEX 4800 Plus MALDI TOF/TOF^{TM}. HR-MS spectra were recorded on a Thermo Fisher Scientific LTQ FT Ultra Mass Spectrometer. Column chromatography was performed on silica gel H (300 - 400 mesh). UV-vis absorption spectra were recorded on an ultraviolet visible spectrophotometer (Jasco Model V-530, Japan). Fluorescence spectra were measured on a Fluorescence Spectrophotometer (FluoroMax-4, France). Compounds **2a-d** were synthesized according to previous reports.

*4.1.1 General procedure for the synthesis of **3a-d**.*

To a solution of dipyrromethane (392 mg, 2.7 mmol) and compound **2** (2.7 mmol) in distilled CH_2Cl_2 (500 mL) was added dropwise trifluoroacetic acid (0.12 mL, 1.7 mmol) under nitrogen, and the mixture was stirred at room temperature for 12 h. 2,3-Dicyano-5,6-dichlorobenzoquinone (DDQ) (0.735 g, 3.24 mmol) and triethylamine (4 mL) were added, and then the mixture was

continued for 1 h. The solvent was evaporated under reduced pressure and the resulting residue was purified by silica gel chromatography to afford **3a-d** as the purple solid.

*5,15-Di((3-ethoxycarbonylmethoxyl)phenyl)porphin (**3a**).* Above described general method was followed to afford the crude mixture which was purified by silica gel chromatography eluted with CH_2Cl_2 to give the purple solid **3a** (527 mg, 58.6%). ^{1}H NMR (400 MHz, $CDCl_3$): δ ppm 10.33 (s, 2H), 9.40 (d, *J* = 3.5 Hz, 4H), 9.12 (d, 4H), 7.93 (d, *J* = 6.0 Hz, 2H), 7.83 (s, 2H), 7.76-7.70 (m, 2H), 7.40 (d, *J* = 8.1 Hz, 2H), 4.86 (s, 4H), 4.15 (q, *J* = 7.2 Hz, 4H), 1.28 (t, 6H), -3.16 (s, 2H).

*5,15-Di((3-ethoxycarbonylpropoxyl)phenyl)porphin (**3b**).* Above described general method was followed to afford the crude mixture which was purified by silica gel chromatography eluted with dichloromethane/petroleum ether (v/v = 3:1) to give the purple solid **3b** (512 mg, 52.5%). ^{1}H NMR (400 MHz, $CDCl_3$): δ ppm 10.34 (s, 2H), 9.42 (d, *J* = 4.6 Hz, 4H), 9.17 (d, *J* = 4.6 Hz, 4H), 7.91 (d, *J* = 7.4 Hz, 2H), 7.87 (s, 2H), 7.76-7.70 (m, 2H), 7.39 (dd, *J* = 8.3, 1.8 Hz, 2H), 4.27 (t, *J* = 6.1 Hz, 4H), 4.20 (q, *J* = 7.1 Hz, 4H), 2.66 (t, *J* = 7.3 Hz, 4H), 2.31-2.24 (m, 4H), 1.29 (t, *J* = 7.2 Hz, 6H), -3.08 (s, 2H).

*5,15-Di((3-carboxymethoxyl-4-methoxyl)phenyl)porphin (**3c**).* Above described general method was followed to afford the crude mixture which was purified by silica gel chromatography eluted with dichloromethane/petroleum ether (v/v = 3:1) to give the purple solid **3c** (500 mg, 51.0%). ^{1}H NMR (400 MHz, $CDCl_3$): δ ppm 10.31 (s, 2H), 9.39 (d, *J* = 4.6 Hz, 4H), 9.13 (d, *J* = 4.6 Hz, 4H), 7.89-7.83 (m, 2H), 7.78 (t, *J* = 2.3 Hz, 2H), 7.33 (dd, *J* = 8.2, 1.9 Hz, 2H), 4.90 (s, 4H), 4.25 (q, *J* = 7.1 Hz, 4H), 4.21 (s, 6H), 1.18 (t, *J* = 7.1 Hz, 6H), -3.10 (s, 2H).

*5,15-Di((3-ethoxycarbonylpropoxyl-4-methoxyl)phenyl)porphin (**3d**).* Above described general method was followed to afford the crude mixture which was purified by silica gel

chromatography eluted with CH_2Cl_2 to give the purple solid **3d** (485.8 mg, 46.1%). ^{1}H NMR (400 MHz, $CDCl_3$): δ ppm 10.30 (s, 2H), 9.39 (d, *J* = 4.6 Hz, 4H), 9.15 (d, *J* = 4.6 Hz, 4H), 7.90-7.83 (m, 2H), 7.81 (d, *J* = 8.1 Hz, 2H), 7.29 (d, *J* = 8.1 Hz, 2H), 4.24 (t, *J* = 6.3 Hz, 4H), 4.17 (s, 6H), 4.10 (q, *J* = 7.2 Hz, 4H), 2.62 (t, *J* = 7.4 Hz, 4H), 2.27 (m, *J* = 6.9 Hz, 4H), 1.20 (t, *J* = 7.1 Hz, 6H), -3.07 (s, 2H).

*4.1.2 General procedure for the synthesis of **P1-4**.*

Porphin **3** (0.5 mmol) was dissolved in tetrahydrofuran/methanol (100 mL, v/v = 1/1) followed by 2 N KOH (25 mL). The reaction mixture was stirred under reflux for 12 h under nitrogen. After the reaction solution was cooled to room temperature, the solvent was evaporated under reduced pressure. The residue was dissolved in water (30 mL) and the pH was adjusted to 3-4 with 1 N HCl. The product (**P1-4**) was precipitated, collected by filtration and dried.

*5,15-Di((3-carboxymethoxyl)phenyl)porphin (**P1**).* **P1** was prepared by following the above general procedure (276.4 mg, 90.6%). ^{1}H NMR (400 MHz, DMSO-d_6): δ ppm 10.57 (s, 2H), 9.59 (d, *J* = 4.1 Hz, 4H), 9.09 (d, *J* = 3.4 Hz, 4H), 7.96-7.67 (m, 6H), 7.44 (d, *J* = 7.9 Hz, 2H), 4.89 (s, 4H), -3.27 (s, 2H). ^{13}C NMR (100 MHz, DMSO-d_6): δ ppm 171.31, 157.40, 146.80, 145.21, 142.04, 133.02, 131.26, 128.59, 128.33, 121.52, 118.85, 114.92, 106.20, 65.99. HRMS (MALDI-TOF): m/z calcd for $C_{36}H_{27}N_4O_6$ $[M+H]^+$, 611.1925; found, 611.1926.

*5,15-Di((3-carboxypropoxyl)phenyl)porphin (**P2**).* **P2** was prepared by following the above general procedure (313.2 mg, 94.2%). ^{1}H NMR (400 MHz, DMSO-d_6): δ ppm 12.21 (s, 2H), 10.61 (s, 2H), 9.63 (d, 4H), 9.09 (d, 4H), 7.89-7.70 (m, 6H), 7.44 (s, 2H), 4.23 (t, 4H), 2.49 (t, J = 8.4 Hz, 4H), 2.14-2.00 (m,4H), -3.28 (s, 2H). ^{13}C NMR (100 MHz, DMSO-d_6): δ ppm 174.68, 157.78, 146.84, 145.28, 142.29, 133.01, 131.27, 128.65, 128.02, 121.52, 118.92, 114.75, 106.20,

67.45, 30.75, 24.89. HRMS (MALDI-TOF): m/z calcd for $C_{40}H_{35}N_4O_6$ $[M+H]^+$, 667.2551; found, 667.2546.

*5,15-Di((3-carboxymethoxyl-4-methoxyl)phenyl)porphin (**P3**).* **P3** was prepared by following the above general procedure (328.4 mg, 98.3%). ^{1}H NMR (400 MHz, DMSO-d_6): δ ppm 10.61 (s, 2H), 9.64 (d, *J* = 3.9 Hz, 4H), 9.13 (d, *J* = 3.7 Hz, 4H), 7.86-7.75 (m, 4H), 7.46 (d, *J* = 6.4 Hz, 2H), 4.92 (s, 4H), 4.09 (s, 6H), -3.21 (s, 2H). ^{13}C NMR (100 MHz, DMSO-d_6): δ ppm 170.98, 149.42, 147.24, 146.34, 145.09, 132.97, 131.36, 128.95, 120.89, 120.64, 118.99, 111.65, 106.13, 65.61, 56.34. HRMS (MALDI-TOF): m/z calcd for $C_{38}H_{31}N_4O_8$ $[M+H]^+$, 671.2136; found, 671.2139.

*5,15-di((3-carboxypropoxyl-4-methoxyl)phenyl)porphin (**P4**).* **P4** was prepared by following the above general procedure (354.4 mg, 97.7%). ^{1}H NMR (400 MHz, DMSO-d_6): δ ppm 12.14 (s, 2H), 10.60 (s, 2H), 9.63 (d, *J* = 4.7 Hz, 4H), 9.12 (d, *J* = 4.6 Hz, 4H), 7.98-7.86 (m, 2H), 7.77 (d, *J* = 7.9 Hz, 2H), 7.45 (d, *J* = 8.1 Hz, 2H), 4.17 (t, *J* = 6.1 Hz, 4H), 4.09 (s, 6H), 2.44 (t, *J* = 7.4 Hz, 4H), 2.12-1.95 (m, 4H), -3.22 (s, 2H). ^{13}C NMR (100 MHz, DMSO-d_6): δ ppm 174.62, 149.61, 147.25, 147.02, 145.11, 133.33, 132.89, 131.36, 128.28, 120.52, 119.11, 111.36, 106.07, 68.14, 56.33, 30.62, 24.92. HRMS (MALDI-TOF): m/z calcd for $C_{42}H_{39}N_4O_8$ $[M+H]^+$, 727.2762; found, 727.2763.

*4.1.3 General procedure for the synthesis of **4a-d**.*

A solution of compound **3** (0.5 mmol) and K_2CO_3 (828 mg, 6 mmol) dissolved in pyridine (23 mL) was heated to reflux under nitrogen, and then 0.5 M *p*-toluenesulfonyl hydrazide in pyridine (0.5 ml) was added every half hour in 16 batches over 8 h. The reaction mixture was cooled to room temperature followed by the addition of ethyl acetate (100 mL) and distilled water (50 mL) and stirred under reflux for 1 h. After cooling and stratification, the organic phase

was washed with saturated brine (50 mL × 3), dried over anhydrous Na_2SO_4 and filtered. The filtrate was stirred at room temperature and chloranil (125 mg) was added in portions. The reaction was stopped when the absorbance peak at 735 nm disappeared. The reaction mixture was washed with 5% $NaHSO_3$ solution (50 mL × 3), water (50 mL × 3), 2 N NaOH (10 mL × 3) and saturated brine (50 mL × 3), dried over anhydrous Na_2SO_4, filtered, and evaporated under reduced pressure. The residue was purified by column chromatography to afford **4a-d** as dark green solid.

*5,15-Di((3-ethoxycarbonylmethoxyl)phenyl)chlorin (**4a**).* Above described general method was followed to afford the crude mixture which was purified by silica gel chromatography eluted with dichloromethane/petroleum ether (v/v = 1:1) to give the green solid **4a** (121 mg, 36.2%). ^{1}H NMR (400 MHz, $CDCl_3$): δ ppm 9.85 (s, 1H), 9.10 (d, *J* = 4.6 Hz, 1H), 8.99 (s, 1H), 8.97 (d, *J* = 4.3 Hz, 1H), 8.87 (d, *J* = 4.7 Hz, 1H), 8.82 (d, *J* = 4.7 Hz, 1H), 8.67 (d, *J* = 4.2 Hz, 1H), 8.41 (d, *J* = 4.6 Hz, 1H), 7.83 (d, *J* = 7.4 Hz, 1H), 7.74 (s, 1H), 7.65 (q, *J* = 8.4 Hz, 2H), 7.54 (d, *J* = 7.4 Hz, 1H), 7.49 (s, 1H), 7.35 (d, *J* = 8.3 Hz, 1H) , 7.27 (d, *J* = 8.3 Hz, 1H), 4.82 (d, *J* = 8.4 Hz, 4H), 4.65 (q, *J* = 7.8 Hz, 2H), 4.37-4.27 (m, 6H), 1.29 (t, *J* = 7.1 Hz, 6H), -1.44 (s, 1H), -1.96 (s, 1H).

*5,15-Di((3-ethoxycarbonylpropoxyl)phenyl)chlorin (**4b**).* Above described general method was followed to afford the crude mixture which was purified by silica gel chromatography eluted with dichloromethane/petroleum ether (v/v = 3:1) to give the green solid **4b** (200 mg, 55.2%). ^{1}H NMR (400 MHz, $CDCl_3$): δ ppm 9.87 (s, 1H), 9.12 (d, *J* = 4.7 Hz, 1H), 9.02 (s, 1H), 8.99 (d, *J* = 4.2 Hz, 1H), 8.89 (d, *J* = 4.7 Hz, 1H), 8.82 (d, *J* = 4.7 Hz, 1H), 8.72 (d, *J* = 3.2 Hz, 1H), 8.46 (d, *J* = 4.6 Hz, 1H), 7.81 (d, *J* = 7.5 Hz, 1H), 7.76 (s, 1H), 7.66 (q, *J* = 7.7 Hz, 2H), 7.53-7.48 (m, 2H), 7.32 (dd, *J* = 8.3, 2.4 Hz, 1H), 7.25 (dd, *J* = 8.4, 2.5 Hz, 1H), 4.69 (t, *J* = 7.7 Hz, 2H), 4.43-

4.36 (m, 2H), 4.25-4.17 (m, 8H), 2.64 (td, *J* = 7.3, 3.7 Hz, 4H), 2.28-2.22 (m, 4H), 1.30 (td, *J* = 7.1, 1.5 Hz, 6H), -1.42 (s, 1H), -1.92 (s, 1H).

5,15-Di((3-ethoxycarbonylmethoxyl-4-methoxyl)phenyl)chlorin ***(4c)***. Above described general method was followed to afford the crude mixture which was purified by silica gel chromatography eluted with dichloromethane /petroleum ether (v/v = 6:1) to give the green solid **4c** (60.1 mg, 16.5%). ^{1}H NMR (400 MHz, $CDCl_3$): δ ppm 9.86 (s, 1H), 9.15 (s, 1H), 9.06-8.95 (m, 2H), 8.91-8.79 (m, 2H), 8.69 (d, *J* = 4.2 Hz, 1H), 8.43 (d, *J* = 4.6 Hz, 1H), 7.84-7.74 (m, 1H), 7.69 (s, 1H), 7.51 (m, 1H), 7.41 (s, 1H), 7.31-7.24 (m, 2H), 4.87 (d, *J* = 9.8 Hz, 4H), 4.69 (t, *J* = 7.5 Hz, 2H), 4.37 (t, *J* = 6.6 Hz, 2H), 4.28-4.22 (m, 4H), 4.18 (d, *J* = 8.8 Hz, 6H), 1.21 (q, *J* = 7.0 Hz, 6H), -1.43 (s, 1H), -1.92 (s, 1H).

5,15-Di((3-ethoxycarbonylpropoxyl-4-methoxyl)phenyl)chlorin ***(4d)***. Above described general method was followed to afford the crude mixture which was purified by silica gel chromatography eluted with CH_2Cl_2 to give the green solid **4d** (56.9 mg, 14.5%). ^{1}H NMR (400 MHz, $CDCl_3$): δ ppm 9.88 (s, 1H), 9.18 (d, *J* = 4.7 Hz, 1H), 9.09-8.99 (m, 2H), 8.93-8.81 (m, 2H), 8.74 (d, *J* = 3.6 Hz, 1H), 8.48 (d, *J* = 4.6 Hz, 1H), 7.81-7.76 (m, 1H), 7.63-7.48 (m, 4H), 7.32-7.27 (m, 1H), 4.74 (t, *J* = 7.8 Hz, 2H), 4.41-4.32 (m, 2H), 4.32-4.23 (m, 8H), 4.19 (d, *J* = 8 Hz, 6H), 2.64 (q, *J* = 7.3, 4H), 2.27-2.19 (m, 4H), 1.23 (t, *J* = 4 Hz, 6H), -1.41 (s, 1H), -1.88 (s, 1H).

4.1.4 General procedure for the synthesis of ***C1-4***.

Compound **4** (0.5 mmol) was dissolved in tetrahydrofuran/methanol (100 mL, v/v = 1/1) followed by 2 N KOH (25 mL). The reaction mixture was stirred under reflux for 12 h under nitrogen. After the reaction solution was cooled to room temperature, the solvent was evaporated

under reduced pressure. The residue was dissolved in water (30 mL) and the pH was adjusted to 3-4 with 1 N HCl. The product (**C1-4**) was precipitated, filtered and dried.

*5,15-Di((3-carboxymethoxyl)phenyl)chlorin (**C1**).* **C1** was prepared by following the above general procedure (280.4 mg, 91.6%). ^{1}H NMR (400 MHz, DMSO-d_6): δ ppm 9.87 (s, 1H), 9.13 (d, *J* = 4.6 Hz, 1H), 9.02 (s, 1H), 8.99 (d, *J* = 4.3 Hz, 1H), 8.87 (d, *J* = 4.7 Hz, 1H), 8.82 (d, *J* = 4.7 Hz, 1H), 8.69 (d, *J* = 4.2 Hz, 1H), 8.43 (d, *J* = 4.6 Hz, 1H), 7.86 (d, *J* = 7.4 Hz, 1H), 7.77 (d, *J* = 2.5 Hz, 1H), 7.68 (q, *J* = 8.4 Hz, 2H), 7.57 (d, *J* = 7.4 Hz, 1H), 7.51 (d, *J* = 2.6 Hz, 1H), 7.37 (dd, *J* = 8.3, 2.4 Hz, 1H), 7.30 (d, *J* = 2.5 Hz, 1H), 4.84 (d, *J* = 8.4 Hz, 4H), 4.68 (t, *J* = 7.9 Hz, 2H), 4.35 (dqd, *J* = 10.7, 7.7, 7.1, 4.2 Hz, 6H), 1.32 (t, *J* = 7.1 Hz, 6H), -1.41 (s, 1H), -1.94 (s, 1H). ^{13}C NMR (100 MHz, DMSO-d_6): δ ppm 171.19, 171.12, 168.11, 168.06, 158.08, 157.31, 152.58, 150.37, 142.95, 142.1, 140.53, 139.33, 135.38, 133.71, 133.60, 131.66, 129.53, 129.30, 128.63, 128.35, 127.56, 125.48, 125.31, 123.03, 120.63, 118.84, 114.76, 114.49, 111.67, 108.85, 97.63, 65.67, 65.61, 35.71, 35.32. HRMS (MALDI-TOF): m/z calcd for $C_{36}H_{29}N_4O_6$ $[M+H]^+$, 613.2082; found, 613.2079.

*5,15-Di((3-carboxypropoxyl)phenyl)chlorin (**C2**).* **C2** was prepared by following the above general procedure (325.8 mg, 97.5%). ^{1}H NMR (400 MHz, DMSO-d_6): δ ppm 12.28 (s, 2H), 10.13 (s, 1H), 9.43 (dd, *J* = 4.8, 1.8 Hz, 1H), 9.26 (s, 1H), 9.13 (d, *J* = 4.2 Hz, 2H), 8.90 (d, *J* = 4.7 Hz, 1H), 8.63 (d, *J* = 4.3 Hz, 1H), 8.46 (dd, *J* = 4.7, 1.7 Hz, 1H), 7.81-7.71 (m, 4H), 7.61 (d, *J* = 2.3 Hz, 1H), 7.56 (d, *J* = 7.4 Hz, 1H), 7.46 (dt, *J* = 5.9, 3.0 Hz, 1H), 7.38 (dd, *J* = 8.4, 2.5 Hz, 1H), 4.71 (t, *J* = 8.0 Hz, 2H), 4.47-4.23 (m, 6H), 2.61-2.57 (m, 2H), 2.53 (d, *J* = 7.2 Hz, 2H), 2.18-2.10 (m, 4H), -1.46 (s, 1H), -2.00 (s, 1H). ^{13}C NMR (100 MHz, DMSO-d_6): δ ppm 174.64, 168.20, 168.11, 158.67, 157.79, 152.60, 150.40, 143.16, 142.28, 140.59, 139.42, 135.39, 133.76, 133.59,131.64, 129.66, 129.34, 128.66, 128.41, 127.15, 125.32, 125.23, 123.09, 120.71, 120.63,

118.83, 114.60, 114.44, 111.80, 108.86, 97.68, 67.36, 67.27, 35.80, 35.44, 30.70, 30.67, 24.86, 24.83. HRMS (MALDI-TOF): m/z calcd for $C_{40}H_{37}N_4O_6$ $[M+H]^+$, 669.2708; found, 669.2709.

*5,15-Di((3-carboxymethoxyl-4-methoxyl)phenyl)chlorin (**C3**).* **C3** was prepared by following the above general procedure (324 mg, 96.4%). ^{1}H NMR (400 MHz, DMSO-d_6): δ ppm 10.03 (s, 1H), 9.35 (s, 1H), 9.20 (s, 1H), 9.08-9.01 (m, 2H), 8.86 (d, *J* = 3.7 Hz, 1H), 8.59 (d, *J* = 3.9 Hz, 1H), 8.41 (d, *J* = 3.7 Hz, 1H), 7.68 (s, 2H), 7.48 (d, *J* = 4.2 Hz, 2H), 7.40 (d, *J* = 24.2 Hz, 2H), 4.81 (d, *J* = 19.8 Hz, 4H), 4.66 (t, *J* = 7.5 Hz, 2H), 4.37-4.28 (m, 2H), 4.05 (d, *J* = 14.6 Hz, 6H), -1.48 (s, 1H), -2.07 (s, 1H). ^{13}C NMR (100 MHz, DMSO-d_6): δ ppm 172.31, 163.78, 162.33, 153.61, 153.05, 148.83, 148.79, 146.09, 144.54, 143.78, 133.80, 133.40, 132.73, 132.10, 132.08, 130.94, 129.96, 125.59, 125.28, 125.15, 125.06, 121.28, 116.98, 114.05, 113.75, 113.53, 113.24, 113.13, 105.56, 101.44, 65.12, 59.91, 33.45, 31.80. HRMS (MALDI-TOF): m/z calcd for $C_{38}H_{33}N_4O_8$ $[M+H]^+$, 673.2293; found, 673.2301.

*5,15-Di((3-carboxypropoxyl-4-methoxyl)phenyl)chlorin (**C4**).* **C4** was prepared by following the above general procedure (345.2 mg, 94.7%). ^{1}H NMR (400 MHz, DMSO-d_6): δ ppm 12.31 (s, 2H), 10.31 (s, 1H), 9.67 (s, 1H), 9.46 (s, 1H), 9.24 (d, *J* = 4.2 Hz, 2H), 9.01 (d, *J* = 4.7 Hz, 1H), 8.73 (d, *J* = 4.3 Hz, 1H), 8.51 (d, *J* = 4.7 Hz, 1H), 7.61 (s, 2H), 7.56 (d, *J* = 2.4 Hz, 1H), 7.46 (d, *J* = 6.4 Hz, 1H), 7.38 (m, 1H), 7.30 (m, 1H), 4.67 (t, *J* = 8.0 Hz, 2H), 4.52-4.31 (m, 6H), 4.12 (d, *J* = 5.8 Hz, 6H), 2.64-2.58 (m, 4H), 2.23-2.16 (m, 4H), -1.53 (s, 1H), -2.07 (s, 1H). ^{13}C NMR (100 MHz, DMSO-d_6): δ ppm 179.56, 163.78, 161.39, 153.67, 150.36, 148.56, 148.29, 146.39, 144.57, 142.88, 133.78, 133.45, 132.76, 132.10, 132.04, 130.98, 129.96, 125.57, 125.31, 125.12, 121.25, 116.92, 113.97, 113.51, 113.09, 113.01, 112.54, 105.56, 101.44, 67.91, 55.91, 55.85, 33.45, 31.80, 30.83, 24.61, 24.57. HRMS (MALDI-TOF): m/z calcd for $C_{42}H_{41}N_4O_8$ $[M+H]^+$, 729.8095; found, 729.8096.

*4.1.5 General procedure for the synthesis of **5a-d**.*

A solution of compound **3** (0.5 mmol) and K_2CO_3 (828 mg, 6 mmol) dissolved in pyridine (23 mL) was heated to reflux under nitrogen, and then 0.5 N *p*-toluenesulfonyl hydrazide in pyridine (0.5 ml) was added every half hour in 24 batches over 12 h. The reaction mixture was cooled to room temperature followed by the addtion of ethyl acetate (100 mL) and distilled water (50 mL) and stirred under reflux for 1 h. After cooling and stratification, the organic phase was washed with saturated brine (50 mL × 3), dried over anhydrous Na_2SO_4 and filtered. The filtrate was evaporated under reduced pressure. The residue was purified by column chromatography to afford dark green solid **5a-d**.

*5,15-Di((3-ethoxycarbonylmethoxyl)phenyl)bacteriochlorin (**5a**).* Above described general method was followed to afford the crude mixture which was was purified by silica gel chromatography eluted with dichloromethane /petroleum ether (v/v = 6:1) to give dark green solid **5a** (95.2 mg, 28.4%). ^{1}H NMR (400 MHz, $CDCl_3$): δ ppm 8.79 (s, 2H), 8.57 (d, 2H), 8.19 (d, *J* = 4.4 Hz, 2H), 7.64-7.59 (m, 2H), 7.52 (d, *J* = 7.5 Hz, 2H), 7.45 (d, *J* = 2.5 Hz, 2H), 7.24 (dd, *J* = 8.4, 2.6 Hz, 2H), 4.80 (s, 4H), 4.55-4.41 (m, 4H), 4.31 (q, *J* = 7.2 Hz, 4H), 4.23-4.10 (m, 4H), 1.32 (t, *J* = 7.1 Hz, 6H), -1.58 (s, 2H).

*5,15-Di((3-ethoxycarbonylpropoxyl)phenyl)bacteriochlorin (**5b**).* Above described general method was followed to afford the crude mixture which was purified by silica gel chromatography eluted with dichloromethane /petroleum ether (v/v = 3:1) to give dark green solid **5b** (125.3 mg, 34.5%). ^{1}H NMR (400 MHz, $CDCl_3$): δ ppm 8.73 (s, 2H), 8.52 (d, 2H), 8.17 (d, 2H), 7.55 (dd, *J* = 8.3, 7.4 Hz, 2H), 7.44-7.38 (m, 4H), 7.16 (ddd, *J* = 8.3, 2.6, 1.0 Hz, 2H), 4.72-3.96 (m, 16H), 2.57 (t, *J* = 7.3 Hz, 4H), 2.21-2.14 (m, 4H), 1.25 (t, *J* = 7.2 Hz, 6H), -1.60 (s, 2H).

*5,15-Di((3-ethoxycarbonylmethoxyl-4-methoxyl)phenyl)bacteriochlorin (**5c**).* Above described general method was followed to afford the crude mixture which was purified by silica gel chromatography eluted with dichloromethane /petroleum ether (v/v = 6:1) to give dark green solid **5c** (96.8 mg, 26.5%). ^{1}H NMR (400 MHz, $CDCl_3$): δ ppm 8.78 (s, 2H), 8.56 (d, *J* = 4.2 Hz, 2H), 8.20 (d, *J* = 4.2 Hz, 2H), 7.48 (q, *J* = 3.6 Hz, 2H), 7.36 (t, *J* = 2.5 Hz, 2H), 7.22 (d, *J* = 8.2 Hz, 2H), 4.83 (s, 4H), 4.49 (t, *J* = 8.3 Hz, 4H), 4.22 (dq, *J* = 13.4, 7.2 Hz, 8H), 4.14 (s, 6H), 1.22 (t, *J* = 7.1 Hz, 6H), -1.57 (s, 2H).

*5,15-Di((3-ethoxycarbonylpropoxyl-4-methoxyl)phenyl)bacteriochlorin (**5d**).* Above described general method was followed to afford the crude mixture which was purified by silica gel chromatography eluted with CH_2Cl_2 to give dark green solid **5d** (72.5 mg, 18.4%). ^{1}H NMR (400 MHz, $CDCl_3$): δ ppm 8.78 (s, 2H), 8.56 (d, *J* = 4.5 Hz, 2H), 8.21 (d, 2H, *J* = 4.5 Hz), 7.44-7.39 (m, 4H),7.24 (d, *J* = 7.8 Hz, 2H), 7.19 (d, *J* = 8.1 Hz, 2H), 4.49 (t, *J* = 8.3 Hz, 4H), 4.23-4.09 (m, 18H), 2.60 (t, *J* = 7.3 Hz, 4H), 2.24 (p, *J* = 6.9 Hz, 4H), 1.22 (t, *J* = 7.1 Hz, 6H), -1.56 (s, 2H).

*4.1.6 General procedure for the synthesis of **B1-4**.*

Compound **5** (0.5 mmol) was dissolved in tetrahydrofuran/methanol (100 mL, v/v = 1/1) followed by 2 N KOH (25 mL). The reaction mixture was stirred under reflux for 18 h under nitrogen. After the reaction solution was cooled to room temperature, the solvent was evaporated under reduced pressure. The residue was dissolved in water (30 mL) and the pH was adjusted to 3-4 with 1 N HCl. The product (**B1-4**) was precipitated, filtered and dried.

*5,15-Di((3-carboxymethoxyl)phenyl]bacteriochlorin (**B1**).* **B1** was prepared by following the above general procedure (299.7 mg, 97.6%). ^{1}H NMR (400 MHz, DMSO-d_6): δ ppm 13.08 (s, 2H), 8.91 (s, 2H), 8.74 (d, *J* = 4.5 Hz, 2H), 8.10 (d, *J* = 4.5 Hz, 2H), 7.64 (t, *J* = 7.8 Hz, 2H),

7.52-7.40 (m, 4H), 7.24 (d, *J* = 8.4 Hz, 2H), 4.85 (s, 4H), 4.45 (t, *J* = 8.4 Hz, 4H), 4.12 (qt, *J* = 16.9, 8.0 Hz, 4H), -1.65 (s, 2H). ^{13}C NMR (100 MHz, DMSO-d_6): δ ppm 170.81, 162.65, 162.15, 157.83, 143.29, 136.39, 135.12, 129.45, 125.35, 122.96, 121.81, 118.46, 114.38, 113.70, 100.03, 65.21, 34.97, 34.75. HRMS (MALDI-TOF): m/z calcd for $C_{36}H_{30}N_4O_6$ $[M]^+$, 614.2160; found, 614.2163.

*5,15-Di((3-carboxypropoxyl)phenyl)bacteriochlorin (**B2**)*. **B2** was prepared by following the above general procedure (297 mg, 88.6%). ^{1}H NMR (400 MHz, DMSO-d_6): δ ppm 12.16 (s, 2H), 8.90 (s, 2H), 8.73 (d, *J* = 4.5 Hz, 2H), 8.10 (d, *J* = 4.5 Hz, 2H), 7.62 (t, *J* = 7.8 Hz, 2H), 7.42 (d, *J* = 9.2 Hz, 4H), 7.30-7.21 (m, 2H), 4.44 (t, *J* = 8.4 Hz, 4H), 4.24-4.02 (m, 8H), 2.44 (t, *J* = 7.3 Hz, 4H), 2.02 (p, *J* = 6.9 Hz, 4H), -1.66 (s, 2H). ^{13}C NMR (100MHz, DMSO-d_6): δ ppm 174.64, 162.62, 162.14, 158.56, 143.41, 136.42, 135.11, 129.48, 124.90, 122.92, 121.83, 118.50, 114.25, 113.81, 99.99, 67.26, 34.96, 34.77, 30.69, 24.85. HRMS (MALDI-TOF): m/z calcd for $C_{40}H_{38}N_4O_6$ $[M]^+$, 670.2786; found, 670.2780.

*5,15-Di((3-carboxymethoxyl-4-methoxyl)phenyl)bacteriochlorin (**B3**)*. **B3** was prepared by following the above general procedure (312 mg, 92.6%). ^{1}H NMR (400 MHz, DMSO-d_6): δ ppm 12.02 (s, 2H), 8.90 (s, 2H), 8.72 (d, *J* = 3.9 Hz, 2H), 8.13 (d, *J* = 3.7 Hz, 4H), 7.49 (s, 2H), 7.36 (d, *J* = 6.4 Hz, 2H), 7.28 (d, *J* = 8.2 Hz, 2H), 4.78 (s, 4H), 4.34-4.18 (m, 4H), 4.09 (s, 6H), -1.64 (s, 2H). ^{13}C NMR (100 MHz, DMSO-d_6): δ ppm 175.31, 163.88, 162.38, 160.46, 153.68, 152.05, 148.01, 146.09, 142.75, 134.50, 133.56, 132.04, 128.58, 125.67, 125.32, 124.39, 117.92, 114.74, 113.48, 102.92, 61.82, 58.94, 33.45, 31.93. HRMS (MALDI-TOF): m/z calcd for $C_{38}H_{34}N_4O_8$ $[M]^+$, 674.2371; found, 674.2370.

*5,15-Di((3-carboxypropoxyl-4-methoxyl)phenyl)bacteriochlorin (**B4**)*. **B4** was prepared by following the above general procedure (327.2 mg, 89.6%). ^{1}H NMR (400 MHz, DMSO-d_6): δ

ppm 12.08 (s, 2H), 8.89 (s, 2H), 8.72 (d, *J* = 4.6 Hz, 2H), 8.13 (d, *J* = 4.6 Hz, 2H), 7.48 (s, 2H), 7.37 (d, *J* = 7.7 Hz, 2H), 7.29 (d, *J* = 8.2 Hz, 2H), 4.44 (t, *J* = 8.4 Hz, 4H), 4.22-4.05 (m, 8H), 3.99 (s, 6H), 2.42 (t, *J* = 7.4 Hz, 4H), 2.00 (q, *J* = 7.0 Hz, 4H), -1.65 (s, 2H). ^{13}C NMR (100 MHz, DMSO-d_6): δ ppm 180.36, 163.88, 162.37, 161.41, 154.61, 152.35, 148.29, 146.69, 142.75, 134.50, 133.53, 132.04, 128.38, 125.75, 124.35, 116.02, 113.69, 112.77, 102.92, 67.91, 55.91, 33.45, 32.90, 30.93, 24.87. HRMS (MALDI-TOF): m/z calcd for $C_{42}H_{42}N_4O_8$ $[M]^+$, 730.2997; found, 730.2996.

4.2. Photophysical and photochemical measurements

4.2.1. Absorption and emission spectra.

UV-visible absorption spectra were recorded on an ultraviolet visible spectrophotometer (Model V-530, Japan). Fluorescence spectra were measured on a Fluorescence Spectrophotometer (FluoroMax-4, France). Slits were kept narrow to 1 nm in excitation and 1 or 2 nm in emission. Right angle detection was used. All the measurements were carried out at room temperature. **P1-4**, **C1-4** and **B1-4** were dissolved in DMSO to get different concentration solutions (1-10 μM).

4.2.2. Singlet oxygen generation detection.

The singlet oxygen ability of **P1-4**, **C1-4** and **B1-4** was monitored by chemical oxidation of 1,3-diphenylisobenzofuran (DPBF) in the DMF solution. Typically, 3 mL portions of DMF solution containing 20 μM DPBF and 0.5 μM PSs were placed in a sealed quartz cuvette and respectively irradiated with 635 nm, 650 nm and 730 nm light at the 5 mW/cm^2 laser intensity. The natural logarithm values of absorption of DPBF at 410 nm were plotted against the irradiation time and fit by a first-order linear least squares model to get the singlet oxygen generation rate of the photosensitized process [51].

4.3. Cell studies.

4.3.1. Cell lines and culture conditions

Human esophageal cancer cell line Eca-109 was obtained from the Type Culture Collection of the Chinese Academy of Sciences. All cell culture related reagents were purchased from Shanghai Ming Rong Bio-Science Technology Co., Ltd. Cells were cultured in normal RPMI-1640 culture medium with 10% fetal bovine serum (FBS), 50 units per mL penicillin and 50 mg mL^{-1} streptomycin in 5% CO_2 at 37 ^oC.

4.3.2. MTT cell viability assay

Eca-109 cells were cultured in RPMI-1640 medium with 10% (v/v) FBS, collected with 0.25% (w/v) trypsin, and seeded in 96-well plates at 5×10^4 cells per well. The cells were allowed to attach to the bottom of the wells for 24 hours prior to start the experiment. RPMI-1640 medium containing **P1-4**, **C1-4** and **B1-4** in different concentrations (range from 0 to 60 μM) was administered to cells and allowed to uptake for 24 hours. Nonirradiated cells were used to investigate the dark cytotoxicity. RPMI-1640 medium containing PSs was removed and cells were washed with fresh PBS before irradiation with different concentrations (range from 0 to 16 μM) and light doses (16 J/cm^2) using an Nd : YAG laser at 635 nm, 650 nm and 730 nm. The cell viability was evaluated by 3-(4,5-dimethyl-2-thiazolyl)-2,5-diphenyl- 2H-terazolium bromide (MTT) colorimetric assay 24 hours after treatment. Irradiated cells were used to investigate the phototoxicity.

4.4. Intracellular localization.

The cells were plated on poly-L-lysine coated coverslips in 12-well plates at the density of 1×10^5 cells/mL. After 24 h, the cells were incubated in the dark at 37 ^oC with 10 μM drug for 4 h, and then rinsed in the RPMI-1640 medium, followed by incubation with Mitro-tracker Green

and Lyso-Blue for 20 min at 37 ^{o}C in a 5% CO_2 incubator, respectively. After rinsed three times with PBS, the coverslips were fixed with 4% (w/v) paraformaldehyde at 4 ^{o}C for 30 min. The cells were observed with confocal fluorescence microscopy (Carl Zeiss LSM 700, Jena, Germany). Mitro-tracker Green, Lyso-Blue, and **B2** were respectively excited at the wavelength of 490, 373, 373 nm and the signals from different probes were acquired in a sequential scan mode.

4.5. In vivo experiments

4.5.1. Tumor xenograft mice model.

Four-week-old female BALB/c nude mice were obtained from Shanghai SLAC Laboratory Animal Company and housed in dedicated pathogen-free barrier facilities. The 5×10^6 Eca-109 cells were injected subcutaneously in 200 μL PBS into the right forelimb. All animal protocols were approved by the Animal Care and Use Committee of Donghua University.

4.5.2. In vivo photosensitizing efficacy.

When the tumor reached approximately 100 mm^3 in size (about 14 days after inoculation), 24 tumor-bearing mice were divided into 4 groups: control, light only, **B2** and **B2**-PDT (each group contained 6 mice). PS was injected into the tail vein of mice in the **B2** and **B2**-PDT groups at a dose of 5 mg/kg in 0.2 mL solution via the lateral tail vein. Then the mice were restrained in plastic plexiglass holders without anesthesia and treated with laser light (730 nm, 120 J/cm^2, 180 mW/cm^2) except for the control and **B2** group. The power was monitored during the entire treatment. Post-PDT, the mice were observed daily for tumor regrowth or tumor cure. Visible tumors were measured every two days using two orthogonal measurements L and W (perpendicular to L), and the volumes were calculated using the formula $V = LW^2/2$ and recorded. After **B2**-PDT in 14 days, the tumor was weighed, and tumor inhibition rates were

calculated. The statistical differences between groups with respect to the mean tumor volume were evaluated by using SPSS 19.0 for windows software. The significance was accepted at $P < 0.05$.

Notes

The authors declare no competing financial interest.

Acknowledgment

This work was supported by the Fundamental Research Fund for the Central Universities (No.17D110513), Foundation of Shanghai Science and Technology Committee (No.15431904100, 16ZR1400600, 17PJ1432800, 17431902600, 17430741800, 17430711900, 18430713000), and the Grant of Ningbo Science and Technology Bureau (No.2017BS1CA01008).

Abbreviations used

PDT, photodynamic therapy; ROS, reactive oxygen species; PS, photosensitizer; DDQ, 2,3-dichloro-5,6-dicyano-1,4-benzoquinone; NMR, nuclear magnetic resonance; DPBF, 1,3-diphenylisobenzofuran; CH_2Cl_2, dichloromethane; DMSO, dimethyl sulfoxide; DMF, dimethylformamide; FBS, fetal bovine serum; PBS, phosphate buffered saline; MTT, 3-(4,5-dimethyl-2-thiazolyl)-2,5-diphenyl-2H-terazolium bromide

Supporting Information

Supplementary data associated with this article can be found in the online version. ^{1}H NMR, ^{13}C NMR, HR-MS, UV-visible absorption, ROS formation on photolysis, in vitro dark cytotoxicity and phototoxicity (Fig. **S1-28**).

REFERENCES

[1] Ikeda, A.; Satake, S.; Mae, T.; Ueda, M.; Sugikawa, K.; Shigeto, H.; Funabashi, H.; Kuroda, A. Photodynamic Activities of Porphyrin Derivative-Cyclodextrin Complexes by Photoirradiation. ACS Med. Chem. Lett. 2017, 8 (5), 555-559.

[2] Meng, Z.; Yu, B.; Han, G.; Liu, M.; Shan, B.; Dong, G.; Miao, Z.; Jia, N.; Tan, Z.; Li, B.; Zhang, W.; Zhu, H.; Sheng, C.; Yao, J. Chlorin p(6)-Based Water-Soluble Amino Acid Derivatives as Potent Photosensitizers for Photodynamic Therapy. J. Med. Chem. 2016, 59 (10), 4999-5010.

[3] Liao, P.; Zhang, X.; Zhang, L.; Wang, X.; Zhu, W.; Sun, J.; Yan, Y.; Zhang, L.; Chen, N.; Chen, Z. Synthesis, characterization and biological evaluation of a novel biscarboxymethyl-modified tetraphenylchlorin compound for photodynamic therapy. RSC Adv. 2016, 6 (31), 26186-26191.

[4] Huang, Z. A Review of Progress in Clinical Photodynamic Therapy. Technol. Cancer Res. Treat. 2005, 4 (3), 283-293.

[5] Mironov, A. F.; Grin, M. A.; Pantushenko, I. V.; Majouga, A. G. Synthesis and Investigation of Photophysical and Biological Properties of Novel S-Containing Bacteriopurpurinimides. J. Med. Chem. 2017, 60 (24), 10220-10230.

[6] Zhu, W.; Gao, Y.-H.; Song, C.-H.; Lu, Z.-B.; Namulinda, T.; Han, Y.-P.; Yan, Y.-J.; Wang, L.-X.; Chen, Z.-L. Synthesis and evaluation of new 5-aminolevulinic acid derivatives as prodrugs of protoporphyrin for photodynamic therapy. Photochem. Photobiol. Sci. 2017, 16 (11), 1623-1630.

[7] Pandey, S. K.; Gryshuk, A. L.; Sajjad, M.; Zheng, X.; Chen, Y. H.; Abouzeid, M. M.; Morgan, J.; Charamisinau, I.; Nabi, H. A.; Oseroff, A.; Pandey, R. K. Multimodality agents for tumor imaging (PET, fluorescence) and photodynamic therapy. A possible "see and treat" approach. J. Med. Chem. 2005, 48 (20), 6286-6295.

[8] Kousis, P. C.; Henderson, B. W.; Maier, P. G.; Gollnick, S. O. Photodynamic therapy enhancement of antitumor immunity is regulated by Neutrophils. Cancer Res. 2007, 67 (21), 10501-10510.

[9] Pandey, R. K. Recent advances in photodynamic therapy. J. Porphyrins Phthalocyanines 2000, 4 (4), 368-373.

[10] Brown, S. B.; Brown, E. A.; Walker, I. The present and future role of photodynamic therapy in cancer treatment. Lancet Oncol. 2004, 5 (8), 497-508.

[11] Vicente, M. G. H. Porphyrin-based sensitizers in the detection and treatment of cancer: recent progress. Curr. Med. Chem.: Anti-Cancer Agents 2001, 1 (2), 175-194.

[12] Drogat, N.; Gady, C.; Granet, R.; Sol, V. Design and synthesis of water-soluble polyaminated chlorins and bacteriochlorins - With near-infrared absorption. Dyes Pigm. 2013, 98 (3), 609-614.

[13] Allison, R. R.; Sibata, C. H. Oncologic photodynamic therapy photosensitizers: a clinical review. Photodiagn. Photodyn. Ther. 2010, 7 (2), 61-75.

[14] Bakri, S. J.; Kaiser, P. K. Verteporfin ocular photodynamic therapy. Expert Opin. Pharmacother. 2004, 5 (1), 195-203.

[15] Huggett, M. T.; Jermyn, M.; Gillams, A.; Illing, R.; Mosse, S.; Novelli, M.; Kent, E.; Bown, S. G.; Hasan, T.; Pogue, B. W.; Pereira, S. P. Phase I/II study of verteporfin photodynamic therapy in locally advanced pancreatic cancer. Br. J. Cancer 2014, 110 (7), 1698-1704.

[16] Allison, R. R.; Downie, G. H.; Cuenca, R.; Hu, X.-H.; Childs, C. J. H.; Sibata, C. H. Photosensitizers in clinical PDT. Photodiagn. Photodyn. Ther. 2004, 1 (1), 27-42.

[17] Hargus, J. A.; Fronczek, F. R.; Vicente, M. G. H.; Smith, K. M. Mono-(L)-aspartylchlorin-e6. Photochem. Photobiol. 2007, 83 (5), 1006-1015.

[18] Wagner, A.; Kiesslich, T.; Neureiter, D.; Friesenbichler, P.; Puespoek, A.; Denzer, U. W.; Wolkersdoerfer, G. W.; Emmanuel, K.; Lohse, A. W.; Berr, F. Photodynamic therapy for hilar bile duct cancer: clinical evidence for improved tumoricidal tissue penetration by temoporfin. Photochem. Photobiol. Sci. 2013, 12 (6), 1065-1073.

[19] Yu, Q.; Rodriguez, E. M.; Naccache, R.; Forgione, P.; Lamoureux, G.; Sanz-Rodriguez, F.; Scheglmann, D.; Capobianco, J. A. Chemical modification of temoporfin - a second generation photosensitizer activated using upconverting nanoparticles for singlet oxygen generation. Chem. Commun. (Cambridge, U. K.) 2014, 50 (81), 12150-12153.

[20] Lapouge, K.; Naeveke, A.; Gall, A.; Ivancich, A.; Seguin, J.; Scheer, H.; Sturgis, J. N.; Mattioli, T. A.; Robert, B. Conformation of Bacteriochlorophyll Molecules in Photosynthetic Proteins from Purple Bacteria. Biochemistry 1999, 38 (34), 11115-11121.

[21] Vakrat-Haglili, Y.; Weiner, L.; Brumfeld, V.; Brandis, A.; Salomon, Y.; McLlroy, B.; Wilson, B. C.; Pawlak, A.; Rozanowska, M.; Sarna, T.; Scherz, A. The Microenvironment Effect on the Generation of Reactive Oxygen Species by Pd-Bacteriopheophorbide. J. Am. Chem. Soc. 2005, 127 (17), 6487-6497.

[22] Dabrowski, J. M.; Arnaut, L. G. Photodynamic therapy (PDT) of cancer: from local to systemic treatment. Photochem. Photobiol. Sci. 2015, 14 (10), 1765-1780.

[23] Pereira, M. M.; Monteiro, C. J. P.; Simoes, A. V. C.; Pinto, S. M. A.; Abreu, A. R.; Sa, G. F. F.; Silva, E. F. F.; Rocha, L. B.; Dabrowski, J. M.; Formosinho, S. J.; Simoes, S.; Arnaut, L. G. Synthesis and photophysical characterization of a library of photostable halogenated bacteriochlorins: an access to near infrared chemistry. Tetrahedron 2010, 66 (49), 9545-9551.

[24] Borbas, K. E.; Ruzie, C.; Lindsey, J. S. Swallowtail Bacteriochlorins. Lipophilic Absorbers for the Near-Infrared. Org. Lett. 2008, 10 (10), 1931-1934.

[25] Huang, Y.-Y.; Mroz, P.; Zhiyentayev, T.; Sharma, S. K.; Balasubramanian, T.; Ruzie, C.; Krayer, M.; Fan, D.; Borbas, K. E.; Yang, E.; Kee, H. L.; Kirmaier, C.; Diers, J. R.; Bocian, D. F.; Holten, D.; Lindsey, J. S.; Hamblin, M. R. In Vitro Photodynamic Therapy and Quantitative Structure-Activity Relationship Studies with Stable Synthetic Near-Infrared-Absorbing Bacteriochlorin Photosensitizers. J. Med. Chem. 2010, 53 (10), 4018-4027.

[26] Huang, Y.-Y.; Balasubramanian, T.; Yang, E.; Luo, D.; Diers, J. R.; Bocian, D. F.; Lindsey, J. S.; Holten, D.; Hamblin, M. R. Stable Synthetic Bacteriochlorins for Photodynamic Therapy: Role of Dicyano Peripheral Groups, Central Metal Substitution (2H, Zn, Pd), and Cremophor EL Delivery. ChemMedChem 2012, 7 (12), 2155-2167.

[27] Saavedra, R.; Rocha, L. B.; Dabrowski, J. M.; Arnaut, L. G. Modulation of Biodistribution, Pharmacokinetics, and Photosensitivity with the Delivery Vehicle of a Bacteriochlorin Photosensitizer for Photodynamic Therapy. ChemMedChem 2014, 9 (2), 390-398.

[28] Rocha, L. B.; Gomes-da-Silva, L. C.; Dabrowski, J. M.; Arnaut, L. G. Elimination of primary tumours and control of metastasis with rationally designed bacteriochlorin photodynamic therapy regimens. Eur. J. Cancer 2015, 51 (13), 1822-1830.

[29] Banfi, S.; Caruso, E.; Buccafurni, L.; Murano, R.; Monti, E.; Gariboldi, M.; Papa, E.; Gramatica, P. Comparison between 5,10,15,20-Tetraaryl- and 5,15-Diarylporphyrins as Photosensitizers: Synthesis, Photodynamic Activity, and Quantitative Structure-Activity Relationship Modeling. J. Med. Chem. 2006, 49 (11), 3293-3304.

[30] Bourre, L.; Simonneaux, G.; Ferrand, Y.; Thibaut, S.; Lajat, Y.; Patrice, T. Synthesis, and in vitro and in vivo evaluation of a diphenylchlorin sensitizer for photodynamic therapy. J. Photochem. Photobiol., B 2003, 69 (3), 179-192.

[31] Bruckner, C.; Posakony, J. J.; Johnson, C. K.; Boyle, R. W.; James, B. R.; Dolphin, D.

Novel and improved syntheses of 5,15-Diphenylprophyrin and its dipyrrolic precursors. J. Porphyrins Phthalocyanines 1998, 2 (6), 455-465.

[32] Clarke, O. J.; Boyle, R. W. Selective synthesis of asymmetrically substituted 5,15-diphenylporphyrins. Tetrahedron Lett. 1998, 39 (39), 7167-7168.

[33] Tamaru, S.-i.; Yu, L.; Youngblood, W. J.; Muthukumaran, K.; Taniguchi, M.; Lindsey, J. S. A Tin-Complexation Strategy for Use with Diverse Acylation Methods in the Preparation of 1,9-Diacyldipyrromethanes. J. Org. Chem. 2004, 69 (3), 765-777.

[34] Arumugam, N.; Won, D.-H.; Lee, C.-H. Syntheses of regioselectively functionalized, asymmetric porphyrins via "2+2" condensation. J. Porphyrins Phthalocyanines 2002, 6 (7 & 8), 479-483.

[35] Hayashi, S.; Hirao, A.; Imai, A.; Nakamura, H.; Murata, Y.; Ohashi, K.; Nakata, E. Novel Non-Peptide Nociceptin/Orphanin FQ Receptor Agonist, 1-[1-(1-Methylcyclooctyl)-4-piperidinyl]-2-[(3R)-3-piperidinyl]-1H-benzimidazole: Design, Synthesis, and Structure-Activity Relationship of Oral Receptor Occupancy in the Brain for Orally Potent Antianxiety Drug. J. Med. Chem. 2009, 52 (3), 610-625.

[36] Zamboni, R.; Belley, M.; Champion, E.; Charette, L.; DeHaven, R.; Frenette, R.; Gauthier, J. Y.; Jones, T. R.; Leger, S.; et, a. Development of a novel series of styrylquinoline compounds as high-affinity leukotriene D4 receptor antagonists: synthetic and structure-activity studies leading to the discovery of (±)-3-[[[3-[2-(7-chloro-2-quinolinyl)-(E)-ethenyl]phenyl][[3-(dimethylamino)-3-oxopropyl]thio]methyl]thio]propionic acid. J. Med. Chem. 1992, 35 (21), 3832-3844.

[37] Faulkner, J. K.; Woodcock, D. Some derivatives of isovanillin. J. Chem. Soc. 1962, 4737-4738.

[38] Donuru, V. R.; Vegesna, G. K.; Velayudham, S.; Green, S.; Liu, H. Synthesis and Optical Properties of Red and Deep-Red Emissive Polymeric and Copolymeric BODIPY Dyes. Chem. Mater. 2009, 21 (10), 2130-2138.

[39] Chevalier, F.; Geier, G. R., III; Lindsey, J. S. Acidolysis of intermediates used in the preparation of core-modified porphyrinic macrocycles. J. Porphyrins Phthalocyanines 2002, 6 (3), 186-197.

[40] Whitlock, H. W., Jr.; Hanauer, R.; Oester, M. Y.; Bower, B. K. Diimide reduction of porphyrins. J. Amer. Chem. Soc. 1969, 91 (26), 7485-9.

[41] Liao, P.-Y.; Wang, X.-R.; Gao, Y.-H.; Zhang, X.-H.; Zhang, L.-J.; Song, C.-H.; Zhang, D.-P.; Yan, Y.-J.; Chen, Z.-L. Synthesis, photophysical properties and biological evaluation of β-alkylaminoporphyrin for photodynamic therapy. Bioorg. Med. Chem. 2016, 24 (22), 6040-6047.

[42] Dabrowski, J. M.; Pucelik, B.; Regiel-Futyra, A.; Brindell, M.; Mazuryk, O.; Kyziol, A.; Stochel, G.; Macyk, W.; Arnaut, L. G. Engineering of relevant photodynamic processes through structural modifications of metallotetrapyrrolic photosensitizers. Coord. Chem. Rev. 2016, 325, 67-101.

[43] Girotti, A. W. Photosensitized oxidation of membrane lipids: reaction pathways, cytotoxic effects, and cytoprotective mechanisms. J. Photochem. Photobiol., B 2001, 63 (1-3), 103-113.

[44] Lovell, J. F.; Liu, T. W. B.; Chen, J.; Zheng, G. Activatable Photosensitizers for Imaging and Therapy. Chem. Rev. (Washington, DC, U. S.) 2010, 110 (5), 2839-2857.

[45] Wang, L.-X.; Li, J.-W.; Huang, J.-Y.; Li, J.-H.; Zhang, L.-J.; O'Shea, D.; Chen, Z.-L. Antitumor activity of photodynamic therapy with a chlorin derivative in vitro and in vivo. Tumor Biol. 2015, 36 (9), 6839-6847.

[46] Zhang, L.-J.; Bian, J.; Bao, L.-L.; Chen, H.-F.; Yan, Y.-J.; Wang, L.; Chen, Z.-L.

Photosensitizing effectiveness of a novel chlorin-based photosensitizer for photodynamic therapy in vitro and in vivo. J. Cancer Res. Clin. Oncol. 2014, 140 (9), 1527-1536.

[47] Zhang, L.-J.; O'Shea, D.; Zhang, C.-Y.; Yan, Y.-J.; Wang, L.; Chen, Z.-L. Evaluation of a bacteriochlorin-based photosensitizer's anti-tumor effect in vitro and in vivo. J. Cancer Res. Clin. Oncol. 2015, 141 (11), 1921-1930.

[48] Cloonan, S. M.; Elmes, R. B. P.; Erby, M.; Bright, S. A.; Poynton, F. E.; Nolan, D. E.; Quinn, S. J.; Gunnlaugsson, T.; Williams, D. C. Detailed Biological Profiling of a Photoactivated and Apoptosis Inducing pdppz Ruthenium(II) Polypyridyl Complex in Cancer Cells. J. Med. Chem. 2015, 58 (11), 4494-4505.

[49] Gryshuk, A. L.; Chen, Y.; Potter, W.; Ohulchansky, T.; Oseroff, A.; Pandey, R. K. In Vivo Stability and Photodynamic Efficacy of Fluorinated Bacteriopurpurinimides Derived from Bacteriochlorophyll-a. J. Med. Chem. 2006, 49 (6), 1874-1881.

[50] Chen, Y.; Graham, A.; Potter, W.; Morgan, J.; Vaughan, L.; Bellnier, D. A.; Henderson, B. W.; Oseroff, A.; Dougherty, T. J.; Pandey, R. K. Bacteriopurpurinimides: Highly Stable and Potent Photosensitizers for Photodynamic Therapy. J. Med. Chem. 2002, 45 (2), 255-258.

[51] Spiller, W.; Kliesch, H.; Wohrle, D.; Hackbarth, S.; Roder, B.; Schnurpfeil, G. Singlet oxygen quantum yields of different photosensitizers in polar solvents and micellar solutions. J. Porphyrins Phthalocyanines 1998, 2 (2), 145-158.

- Twelve novel PSs, including porphins (**P1-4**), chlorins (**C1-4**) and bacteriochlorins (**B1-4**), were synthesized and characterized.
- All target compounds exhibited the high phototoxicity and the low dark toxicity towards human esophageal cancer cells (Eca-109 cells).
- Compared with all the other compounds, **B2** showed the highest phototoxicity and the lowest dark toxicity.
- **B2** exhibited best photodynamic antitumor efficacy on BALB/c nude mice bearing Eca-109 tumor.
- **B2** is a powerful and promising antitumor photosensitizer for photodynamic therapy.